

Adaptive modulation in $\text{Ni}_2\text{Mn}_{1.4}\text{In}_{0.6}$ magnetic shape memory Heusler alloy

P. Devi¹, Sanjay Singh^{1*}, Kaustuv Manna¹, E. Suard², V. Petricek³, C. Felser¹, and D. Pandey⁴

¹ Max Planck Institute for Chemical Physics of Solids, Nöthnitzer Strasse 40, D-01187 Dresden, Germany

²Institut Laue-Langevin, BP 156, 38042 Grenoble Cedex 9, France

³Institute of Physics ASCR, Department of Structure Analysis, Na Slovance 2, 182 21 Praha, Czech Republic

⁴School of Materials Science and Technology, Indian Institute of Technology (Banaras Hindu University), Varanasi-221005, India.

Abstract

The origin of incommensurate structural modulation in Ni-Mn based magnetic shape memory Heusler alloys is still an unresolved issue inspite of intense focus on this due to the linkage between high magnetic field induced strain and modulated structure. The presence of non-uniform displacement of atoms from their mean positions and phason broadening of satellite peaks of the modulated structure of the martensite phase in Ni_2MnGa can be explained in terms of the electronic stability model. On the other hand, the alternative model of modulation in such magnetic shape memory alloys based on the concept of adaptivity predicts uniform atomic displacement of all the atoms but there is no experimental evidence for the proof of this concept till now. We present here the results of a combined high resolution synchrotron x-ray powder diffraction (SXRPD) and neutron powder diffraction study using (3+1) D superspace group approach which reveals that the modulation in $\text{Ni}_2\text{Mn}_{1.4}\text{In}_{0.6}$, unlike that in Ni_2MnGa , involves uniform atomic displacement. This provides a direct evidence for the applicability of the adaptive phase model in the $\text{Ni}_2\text{Mn}_{1.4}\text{In}_{0.6}$ system. We have also investigated the magnetic structure of the

martensite phase at 3K which reveals an antiferromagnetic alignment of Mn atoms at the two different crystallographic positions in the unit cell on account of the breaking of the time reversal symmetry. Our study underlines the importance of superspace group analysis using complimentary SXRPD and PND in understanding not only the physics of the origin of modulation but also the magnetic and the modulated ground states of the magnetic shape memory Heusler alloys. It also suggests that the origin of modulated phase may not be universal in different Ni-Mn based magnetic shape memory alloys.

Magnetic shape memory Heusler alloys (MSMAs) in the Ni-Mn-X (X= Ga, In, Sn) systems have enormous potential for technological applications due to a rich variety of properties ranging from generation of extremely large magnetic field induced strain (~10%) to pronounced magnetocaloric and barocaloric effects, large magnetoresistance, anomalous Hall effect and large exchange bias[1-6]. The technologically significant physical properties of these alloys are intimately linked with the coupling between structural and magnetic degrees of freedom below the magneto-structural (martensite) phase transition. Since the modulated crystal structure of martensite phase is known to play an important role in deciding their response to the external magnetic field due to low detwinning stress, there is currently a lot of interest in understanding the origin of the modulated structure of the martensite phase itself[7-17]. Two different models have been proposed in the literature for the origin of modulation in the MSMAs. The first one is the adaptive phase model in which the modulated structure is considered as a nanotwinned state of the Bain distorted phase, which maintains the invariance of the habit plane between the high temperature austenite and the low temperature martensite phase[14, 15]. Commensurate superstructure and uniform atomic displacements are the key manifestations of this model. The second model is in terms of the electronic stability linked with a coupling between transverse acoustic (TA₂) mode and charge density wave[18-20]. Observation of dissimilar (non-uniform) displacement for the different atomic sites and incommensurate nature of modulation cannot be explained by the adaptive phase model but is consistent with the soft phonon mode model [10-12, 21, 22]. It has been suggested that the formation of discommensurations in the form of stacking faults and antiphase boundaries can result into an average incommensurate modulated structure even for the adaptive phase model[14-16]. However, the key feature for distinguishing between the two models for the origin of modulation is the identification of the nature (uniform versus non-uniform) of the atomic displacement.

Recently we have shown that the origin of modulation in Ni_2MnGa shape memory Heusler alloy cannot be explained within the framework of adaptive phase model as the modulated structure has non-uniform atomic displacements[12]. Also the fact that the incommensurate martensite phase results from the incommensurate premartensite phase and not directly from the austenite phase does not support the adaptive phase model[11]. On the other hand, the Ni-Mn-In shape alloys do not show the premartensite (precursor) phase formation and the austenite phase transforms directly to the martensite phase. This suggests that this alloy system may be a model system for investigating the applicability of the adaptive phase modulation through a careful analysis of the modulated structure. In this letter, we present the results of Rietveld analysis of SXRPD and powder neutron diffraction (PND) patterns of $\text{Ni}_2\text{Mn}_{1.4}\text{In}_{0.6}$ using (3+1) D superspace- group approach. Our analysis reveals that the modulated martensite structure of $\text{Ni}_2\text{Mn}_{1.4}\text{In}_{0.6}$ involves uniform atomic displacement with respect to their positions in the Bain distorted basic cell that is consistent with the adaptive phase model. Further, we have found evidence for antiferromagnetic correlations for Mn spins at two different crystallographic positions with full and partial Mn occupancy at low temperatures (3K) using Rietveld analysis of the neutron powder diffraction pattern. This is further supported by isothermal magnetization measurements at 2K that reveals a double hysteresis loop due to a spin flop transition induced by a very low magnetic field 0.05 T.

The details of sample preparation, measurements (magnetization, SXRPD and NPD) and Rietveld refinements are given in the Supplemental Material. The low field (500 Oe) magnetization curves of $\text{Ni}_2\text{Mn}_{1.4}\text{In}_{0.6}$ recorded under ZFC, FCC and FCW conditions at 0.05T in the temperature range 2-400 K are shown in Fig.1a. On cooling, a sharp increase in magnetization is observed at a temperature $T \sim 315$ K due to a ferromagnetic transition, which is followed by a decrease in magnetization at $T \sim 295$ K, which is associated with the first order martensite

transition. A splitting between ZFC and FCC curves below $T \sim 145$ is observed that has been attributed to the coexistence of antiferromagnetic and ferromagnetic exchange interactions in the martensitic phase at low temperatures[23]. The temperature dependent magnetization behavior is in well agreement with the literature[3]. The isothermal magnetization $M(H)$ at 2 K is shown in Fig.1b. The $M(H)$ plot indicates typical antiferromagnetic spin alignment as revealed by the appearance of a double hysteresis loop due to a spin flop transition at a very low magnetic field of ± 0.05 T (indicated by red arrows in the inset of Fig.1b). The bifurcation of the ZFC and FC $M(T)$ plots below ~ 145 K also occurs at the same magnetic field (0.05T) suggesting that the ground state of the sample is antiferromagnetic in the ZFC condition whereas FC sample leads to the ferromagnetic state due to a spin flop AFM to FM transition. Our observations although reveals that the true ground state is antiferromagnetic, both the FM and AFM phases are nearly degenerate in view of the extremely low field that induces the spin flop transition.

We now turn towards the structure of the austenite and martensite phases using SXRPD patterns recorded at 350 K (austenite phase) and 235 K (martensite phase), respectively. In the first step of the structure analysis, we performed the indexing of the powder diffraction patterns by Le Bail profile fitting, which refines the unit cell parameters and profile broadening functions to obtain the best fit between the observed and calculated profiles in the least squares sense. At 350 K, all the observed Bragg peaks could be indexed well with the cubic austenite structure (space group $Fm\bar{3}m$) and the refined lattice parameter turns out to be $6.00483(4)$ Å. The presence of the superstructure peaks like (111) and (200) in the SXRPD pattern (inset of Fig.2a) confirms that the sample has the ordered $L2_1$ structure. At 235 K many more reflections appear and the cubic austenite peaks split into two or more peaks clearly indicating that the structure is no longer cubic. A careful analysis of all the observed low intensity peaks revealed that the martensite structure at 235 K cannot be explained in terms of a

simple Bain distorted unit cell and requires consideration of the modulation of the Bain distorted unit cell as reported in other alloy systems as well [7, 8, 11, 24, 25]. Superspace (3+1) D formalism [26-29] is a powerful tool to investigate these type of complex modulated structures and we employed this formalism to investigate the structure of the modulated martensite phase in $\text{Ni}_2\text{Mn}_{1.4}\text{In}_{0.6}$. Following the superspace group formalism, the SXRPD pattern was divided into two sets of reflections: (1) main reflections corresponding to the Bain distorted basic structure and (2) satellites reflections due to the modulation whose intensity is in general much less than the intensity of the main reflections. All the main reflections corresponding to the basic structure could be indexed with a monoclinic cell with space group $I2/m$ and Le-Bail refinement gave us lattice parameters as $a=4.3983(1) \text{ \AA}$, $b=5.6453(2) \text{ \AA}$, $c=4.3379(1) \text{ \AA}$ and $\beta=92.572(2)^\circ$. After obtaining the cell parameters for the basic structure, the full SXRPD pattern including both the main and the satellite reflections was considered for Le-Bail refinement using the superspace group formalism. The satellite reflection were indexed using a modulation wave vector $q=(0, 0, 1/3)$ and superspace group $I2/m(\alpha 0 \gamma)00$. Although this commensurate wave vector could index many of the satellite reflections but some of the calculated satellite reflections were found to be shifted away from the observed reflection positions, as can be clearly seen in the inset of Fig.2b. Therefore the wave vector \mathbf{q} was allowed to be refined. It is evident from the inset of Fig.2c that an incommensurate modulation wave vector of $q=0.35987(8) c^*=(1/3+\delta) c^*$ (where $\delta=0.02653$ is the degree of incommensuration) is able to index the satellite reflections quite precisely, which were not accounted well with the commensurate wave vector $q=1/3$ (Fig.2b). This indicates that the martensite phase of $\text{Ni}_2\text{Mn}_{1.4}\text{In}_{0.6}$ has an incommensurate 3M like modulation (see Ref.[10] for definition of this notation). Moreover, the SXRPD pattern also shows 2nd order satellites (indicated by blue arrows in Fig.2c). A similar 3M (some times also labelled as 6 M (for definition, see Ref.[10]) modulated martensite structure has been reported

for another Ni-Mn-In shape memory alloy composition with martensite transition temperature higher than the present alloy composition[17]. So far we discussed the result of Le Bail refinements, where the atomic positions were not considered. Now we proceed to discuss the results of the Rietveld refinement, where the atomic positions and atomic modulation functions need to be taken in to account during refinements.

For Rietveld refinement, the average atomic positions used for Ni, Mn and In in the basic structure are: Ni at $4h$ (0.5 0.25 0), Mn at $2a$ (0 0 0) and In at $2d$ (0 0.5 0) Wyckoff positions. The extra Mn atoms occupy the In site ($2d$). Further, the deviation of atoms $u(\bar{x}4)$ from the average structure of the modulation was modelled using a harmonic atomic modulation function:

$$u_j(\bar{x}4) = \sum_{n=1}^{\infty} [A_n^j \sin(2\pi n \bar{x}4) + B_n^j \cos(2\pi n \bar{x}4)], \quad (1)$$

where A_n^j and B_n^j are the Fourier amplitudes of the displacement modulation of the j th atom while “ n ” is the order of the Fourier series, which is taken as equivalent to the order of the satellite reflections[30]. Here, we used $n=2$ for Rietveld refinement because we observed satellites up to the 2nd order. In the refinement, the amplitudes of the atomic modulation function were refined without any constraints for different atomic sites similar to that used in the Ni₂MnGa[12] system. While this refinement yields reasonable fit between the observed and the calculated peak profiles (see Fig.S1 of the supplementary file) but the calculated interatomic distances were found to be physically unrealistic for such intermetallic compounds/alloys. For example, some of the interatomic distances were even less than 2.4 Å whereas the sum of the atomic radii of various pairs of atoms is ≥ 2.5 Å. Since this refinement does not yield physically plausible atomic positions, it was rejected. One of the reasons for such implausible atomic positions is site disorder commonly observed in Ni-Mn based Heusler alloys, which can in turn affect the amplitude of atomic modulation if it is not explicitly accounted for in the refinement. In addition, since Ni and

Mn have similar x-ray atomic scattering factors, the positions of these two atoms is not easily distinguishable by XRD.

To obtain physically realistic interatomic distances for the modulated structure, we therefore carried out refinements of the martensite phase using neutron powder diffraction patterns also as the scattering lengths for Ni and Mn have opposite signs. The results of Rietveld refinement using the neutron powder diffraction pattern of $\text{Ni}_2\text{Mn}_{1.4}\text{In}_{0.6}$ at 300 K (RT) is shown in Fig.3. The refinement was done by considering the atomic positions within the $Fm-3m$ space group. The Ni and Mn atoms occupy the $8c$ (0.25 0.25 0.25) and $4a$ (0 0 0) Wyckoff positions, respectively, while In and extra Mn occupy the $4b$ (0.5 0.5 0.5) Wyckoff positions according to their relative occupancies. In the refinement, we also considered the possibility of anti-site disorder but could not observe any substantial effect. After confirming the absence of any discernible anti-site disorder from the analysis of the RT neutron powder diffraction, we proceed to discuss the refinement of the structure of the martensite phase. The neutron diffraction data for the martensite phase was collected at the lowest possible temperature (3K). To investigate the modulated structure, we employed superspace (3+1)D formalism as for the SXRPD data. In the first step of Rietveld refinement, the refinement was carried out without any constraints on the amplitude or direction of atomic displacements for the atomic modulation functions of the different atoms, similar to that used for the analysis of the SXRPD pattern. While the refinement converged for a non-uniform atomic displacement model, but it led to unreasonable interatomic distances, as shown in Fig.4a for some selected atomic pairs obtained using PND. The interatomic distances given in Fig. 4a obtained from a non-uniform displacement model clearly indicates that the use of PND alone cannot resolve the issue of implausible interatomic distances and the problem lies with the modulation model itself. In the next step, we therefore considered a uniform

displacement model for Rietveld refinement in which the amplitude of modulation for all the atomic sites were constrained to be identical (Table I). The derived interatomic distances from the uniform atomic displacement model shown in the Fig.4b clearly reveals that this model gives physically realistic interatomic distances that are acceptable for the shape memory Heusler compounds/alloys. Thus, our results reveal that the modulation in the martensite phase of $\text{Ni}_2\text{Mn}_{1.4}\text{In}_{0.6}$ involves uniform displacement of atoms and is, therefore, consistent with the predictions of the adaptive modulation model.

After getting the correct atomic modulation model and physically realistic amplitude of atomic displacements, we also investigated the magnetic structure. There were four possible magnetic subgroups of the nuclear superspace group $I2/m(\alpha 0 \gamma)00$ (ie, magnetic superspacegroups or mSSG) obtained after breaking of the time reversal symmetry: (i) $I2/m(\alpha 0 \gamma)00$ (ii) $I2'/m(\alpha 0 \gamma)00$ (iii) $I2/m'(\alpha 0 \gamma)00$ and (iv) $I2'/m'(\alpha 0 \gamma)00$. Of these, only (i) and (iv) allow non-zero magnetic moments. The (i) and (iv) mSSG restrict magnetic moments along the b -axis of the monoclinic cell. Out of these two, Rietveld analysis (Fig.5) reveals that the magnetic structure can be described by $I2/m(\alpha 0 \gamma)00$ mSSG in which the magnitude of the magnetic moments of the fully occupied site ($2a$) and partially occupied site ($2d$) are equal but they are antiferromagnetically correlated. Because of the partial (~40%) occupancy of the $2d$ site by Mn, the structure is ferrimagnetic with a resultant magnetic moment of $1.416 \mu_B$, which in good agreement with the value obtained from the magnetization measurement at 2 K (Fig. 1b). As discussed earlier, the observation of the double hysteresis loop in the isothermal magnetization due to a spin flop transition (inset of Fig.1b) also reveals antiferromagnetic correlation of spins. Thus both the magnetization and neutron results confirm that the low temperature phase of $\text{Ni}_2\text{Mn}_{1.4}\text{In}_{0.6}$ is ferrimagnetic, where Mn atoms are coupled antiferromagnetically but due to the unequal occupancy by Mn the magnetism is not compensated at low temperatures.

To summarise, we have critically evaluated the applicability of two existing models (electronic stability and the nano-twinning based adaptivity models) for the origin of modulation in $\text{Ni}_2\text{Mn}_{1.4}\text{In}_{0.6}$ magnetic shape memory alloy. We carried out Rietveld analysis of high resolution SXRPD and powder neutron diffraction patterns of the austenite and modulated martensite phases of $\text{Ni}_2\text{Mn}_{1.4}\text{In}_{0.6}$ using (3+1) D superspace formalism. We have considered both non-uniform and uniform displacement models of incommensurate modulation in the Rietveld refinement and shown that the nature of modulation in $\text{Ni}_2\text{Mn}_{1.4}\text{In}_{0.6}$ involves uniform atomic displacement of atoms as expected for the model based on adaptivity. Further we have shown that the magnetic structure of the martensite phase at 3K is ferrimagnetic where two Mn atoms at different crystallographic positions are coupled antiferromagnetically. The present study underlines the importance of superspace group analysis of the diffraction data to understand the physics of modulation in magnetic shape memory Heusler alloys.

*sanjay.singh@cpfs.mpg.de

Acknowledgments

The work was financially supported by the ERC AG 291472 'IDEA Heusler! S. S. thanks Alexander von Humboldt foundation, Germany for Research Fellowship. DP thanks the Science and Engineering Research Board of India for the award of J.C. Bose National Fellowship. VP acknowledge support of project No. LO1603 under the Ministry of Education, Youth and Sports National sustainability program I of Czech Republic.

References:

- [1] K. Ullakko, J. K. Huang, C. Kantner, R. C. O'Handley, and V. V. Kokorin, *Appl. Phys. Lett.* **69**, 1966 (1996).
- [2] T. Krenke, E. Duman, M. Acet, E. F. Wassermann, X. Moya, L. Manosa, and A. Planes, *Nat. Mater.* **4**, 450 (2005).
- [3] L. Manosa, D. Gonzalez-Alonso, A. Planes, E. Bonnot, M. Barrio, J.-L. Tamarit, S. Aksoy, and M. Acet, *Nat. Mater.* **9**, 478 (2010).
- [4] I. Dubenko, A. K. Pathak, S. Stadler, N. Ali, Y. Kovarskii, V. N. Prudnikov, N. S. Perov, and A. B. Granovsky, *Phys. Rev. B* **80**, 092408 (2009).
- [5] B. M. Wang, Y. Liu, P. Ren, B. Xia, K. B. Ruan, J. B. Yi, J. Ding, X. G. Li, and L. Wang, *Phys. Rev. Lett.* **106**, 077203 (2011).
- [6] S. Singh, L. Caron, S. W. D'Souza, T. Fichtner, G. Porcari, S. Fabbrici, C. Shekhar, S. Chadov, M. Solzi, and C. Felser, *Adv. Mater.* **28**, 3321 (2016).
- [7] L. Righi, F. Albertini, G. Calestani, L. Pareti, A. Paoluzi, C. Ritter, P. A. Algarabel, L. Morellon, and M. Ricardo Ibarra, *J. Solid State Chem.* **179**, 3525 (2006).
- [8] P. J. Brown, J. Crangle, T. Kanomata, M. Matsumoto, K. U. Neumann, B. Ouladdiaf, and K. R. A. Ziebeck, *J. Phys.: Condens. Matter* **14**, 10159 (2002).
- [9] S. Sanjay, J. Nayak, R. Abhishek, R. Parasmani, H. H. Adrian, S. R. Barman, and P. Dhananjai, *J. Phys.: Condens. Matter* **25**, 212203 (2013).
- [10] S. Singh, S. R. Barman, and D. Pandey, in *Zeitschrift für Kristallographie - Crystalline Materials* (2015), p. 13.
- [11] S. Singh, J. Bednarcik, S. R. Barman, C. Felser, and D. Pandey, *Phys. Rev. B* **92**, 054112 (2015).
- [12] S. Singh, V. Petricek, P. Rajput, A. H. Hill, E. Suard, S. R. Barman, and D. Pandey, *Phys. Rev. B* **90**, 014109 (2014).
- [13] S. W. D'Souza, A. Rai, J. Nayak, M. Maniraj, R. S. Dhaka, S. R. Barman, D. L. Schlagel, T. A. Lograsso, and A. Chakrabarti, *Phys. Rev. B* **85**, 085123 (2012).
- [14] M. E. Gruner, S. Fähler, and P. Entel, *physica status solidi (b)* **251**, 2067 (2014).
- [15] S. Kaufmann, U. K. Rößler, O. Heczko, M. Wuttig, J. Buschbeck, L. Schultz, and S. Fähler, *Phys. Rev. Lett.* **104**, 145702 (2010).
- [16] R. Niemann, U. K. Rößler, M. E. Gruner, O. Heczko, L. Schultz, and S. Fähler, *Adv. Eng. Mater.* **14**, 562 (2012).
- [17] H. Yan, Y. Zhang, N. Xu, A. Senyshyn, H.-G. Brokmeier, C. Esling, X. Zhao, and L. Zuo, *Acta Mater.* **88**, 375 (2015).
- [18] A. Zheludev, S. M. Shapiro, P. Wochner, A. Schwartz, M. Wall, and L. E. Tanner, *Phys. Rev. B* **51**, 11310 (1995).
- [19] A. Zheludev, S. M. Shapiro, P. Wochner, and L. E. Tanner, *Phys. Rev. B* **54**, 15045 (1996).
- [20] U. Stuhr, P. Vorderwisch, V. V. Kokorin, and P. A. Lindgård, *Phys. Rev. B* **56**, 14360 (1997).
- [21] A. Pramanick, X. P. Wang, K. An, A. D. Stoica, J. Yi, Z. Gai, C. Hoffmann, and X. L. Wang, *Phys. Rev. B* **85**, 144412 (2012).
- [22] S. Banik, S. Singh, R. Rawat, P. K. Mukhopadhyay, B. L. Ahuja, A. M. Awasthi, S. R. Barman, and E. V. Sampathkumaran, *J. Appl. Phys.* **106**, 103919 (2009).
- [23] S. Aksoy, M. Acet, P. P. Deen, L. Mañosa, and A. Planes, *Phys. Rev. B* **79**, 212401 (2009).
- [24] S. Singh, K. R. A. Ziebeck, E. Suard, P. Rajput, S. Bhardwaj, A. M. Awasthi, and S. R. Barman, *Appl. Phys. Lett.* **101**, 171904 (2012).
- [25] S. Singh, R. Rawat, and S. R. Barman, *Appl. Phys. Lett.* **99**, 021902 (2011).
- [26] P. De Wolff, *Acta Crystallographica Section A: Crystal Physics, Diffraction, Theoretical and General Crystallography* **30**, 777 (1974).

- [27] P. De Wolff, *Acta Crystallographica Section A: Crystal Physics, Diffraction, Theoretical and General Crystallography* **33**, 493 (1977).
- [28] M. Dusek, V. Petricek, M. Wunschel, R. E. Dinnebier, and S. van Smaalen, *J. Appl. Crystallogr.* **34**, 398 (2001).
- [29] T. Janssen, A. Janner, A. Looijenga-Vos, and P. De Wolff, *Mathematical, Physical and Chemical Tables* (1992).
- [30] S. Van Smaalen, *Incommensurate crystallography* (Oxford University Press, USA, 2007).

Figures:

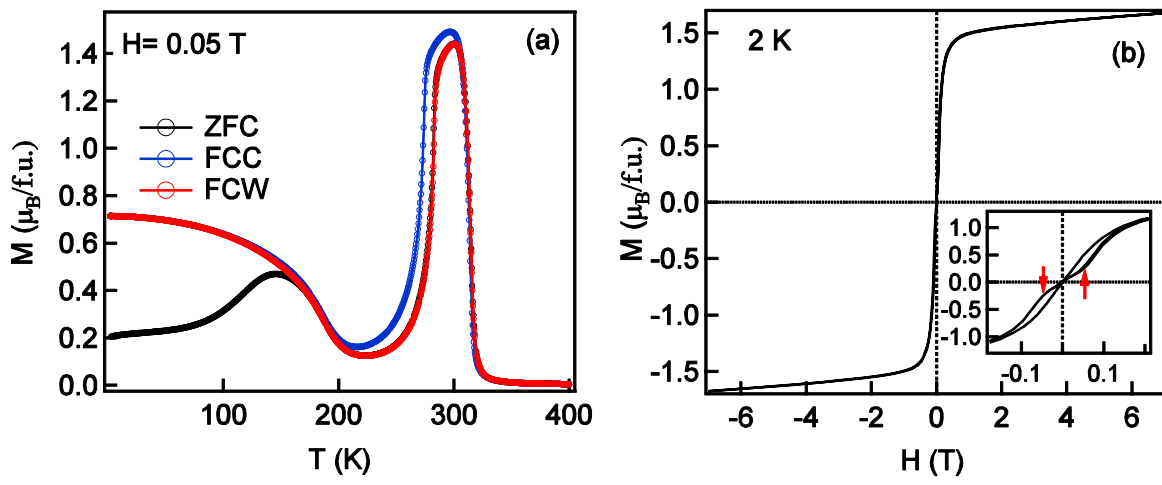


Fig.1: (color online) (a) Magnetization (ZFC, FC and FW) as a function of temperature at 0.05 T and (b) Magnetization as a function of field ($M(H)$) at 2K. Inset shows the $M(H)$ in expanded scale, where metamagnetic (spin-flip) transition are marked by arrows.

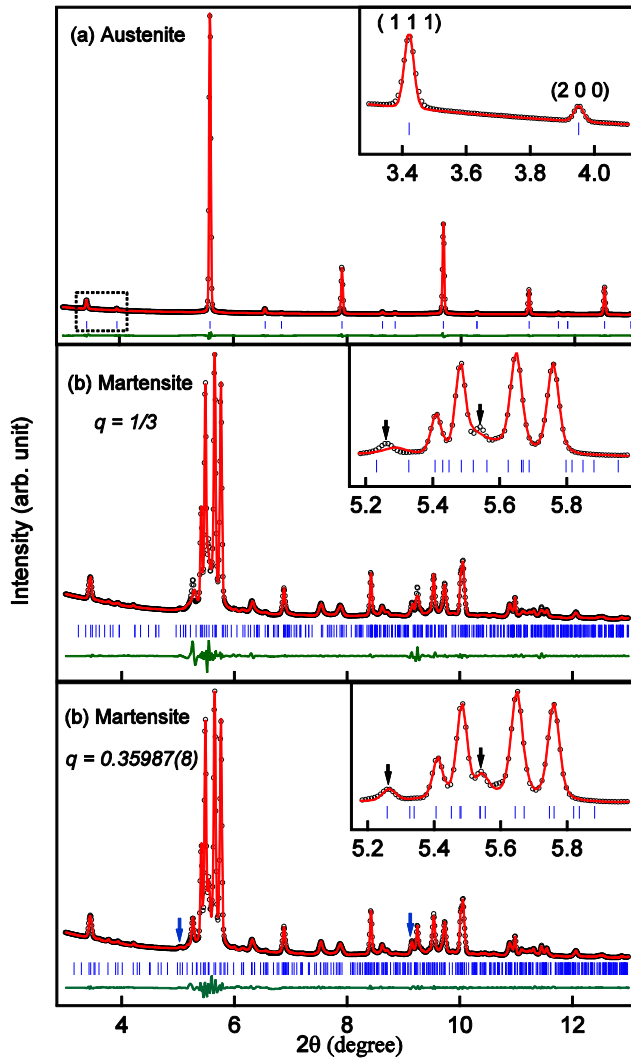


Fig.2: (Color online) Le Bail fits for the SXRPD patterns of $\text{Ni}_2\text{Mn}_{1.4}\text{In}_{0.6}\text{Ga}$ at (a) cubic austenite phase (350 K). Inset shows superlattice reflections related to L_{21} ordering (b) Martensite phase (235 K) with commensurate structure model and (c) Martensite phase (235 K) with incommensurate structure model. The insets show the fit for the main peak region ($2\theta = 5-6^\circ$) on an expanded scale. Arrows in (b) and (c) represent satellite reflections. The experimental data, fitted curve, and the residue are shown by circles (black), continuous line (red), and bottom-most plot (green), respectively. The tick marks (blue) represent the Bragg peak positions.

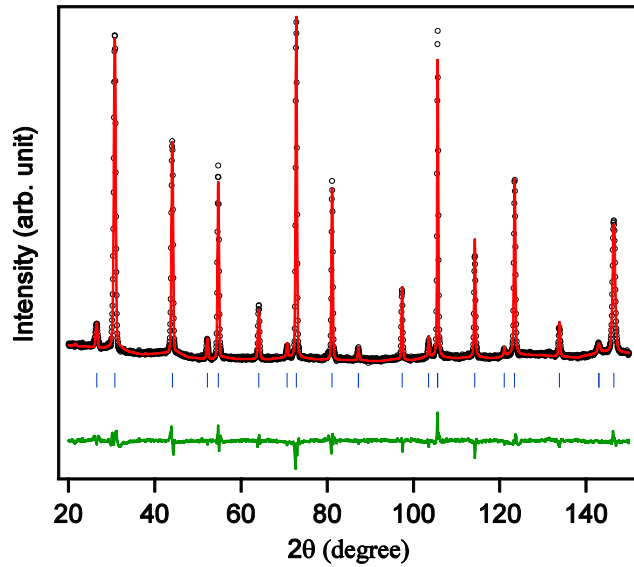


Fig.3: (color online) Rietveld refinement of the neutron powder diffraction pattern at 300 K (austenite phase).

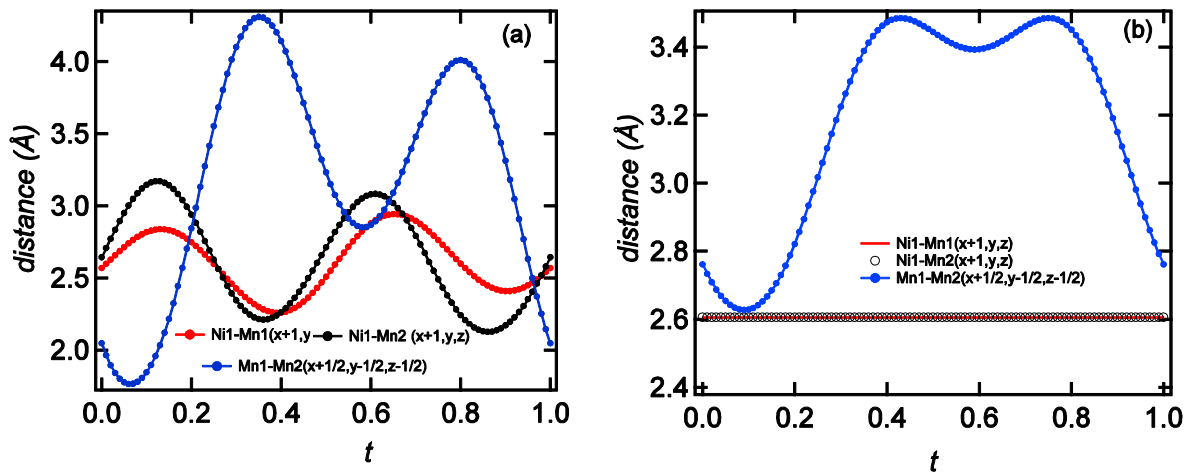


Fig.4: (color online) Distance (selected) as a function of t parameters derived from (a) Non-uniform atomic displacement model (soft phonon mode model) showing unphysical values (less than 2 \AA) and (b) Uniform atomic displacement model (adaptive phase model) showing values that are expected for these kind of intermetallic compounds/alloys.

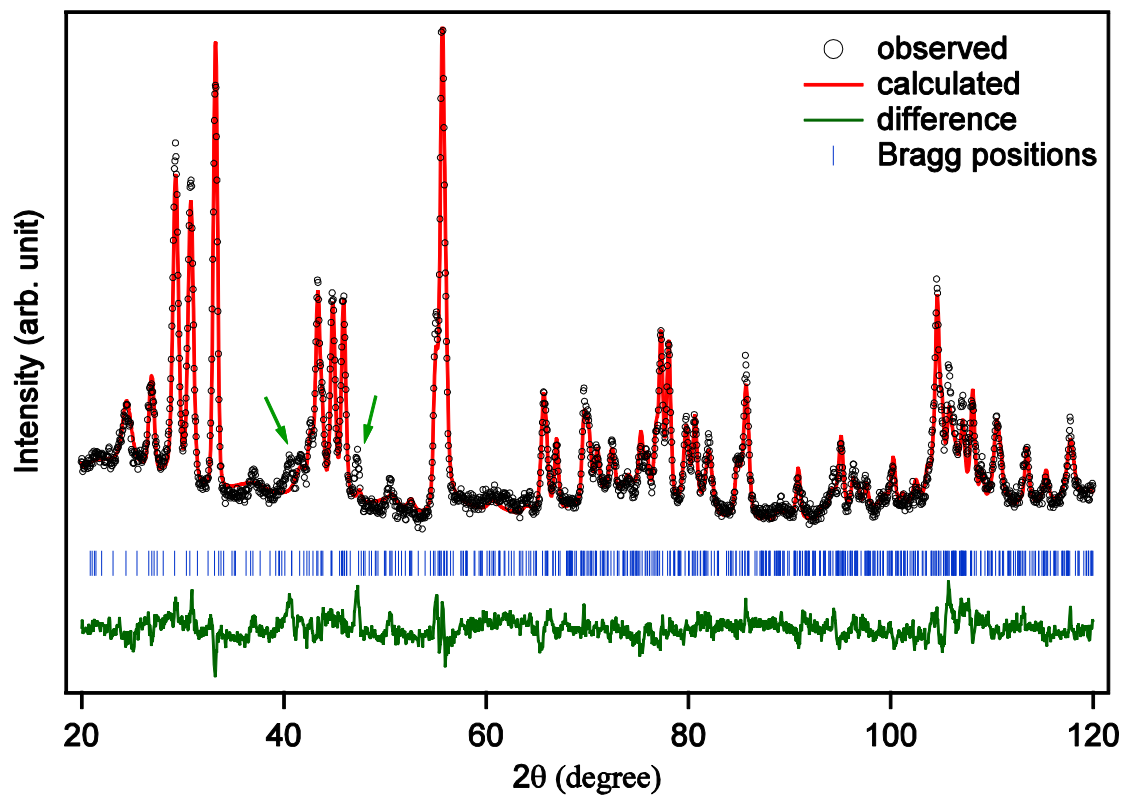


Fig.5: (color online) Observed and calculated neutron diffraction pattern in the martensite phase (3K). Green arrows indicates peaks due to Cryo-furnace wall material (Al).

Table:**Table I :** Atomic positions (x, y, z), atomic displacement parameter (U_{iso}) and amplitudes (A_1, B_1, A_2, B_2) of the modulation function of the modulated martensite phase of $\text{Ni}_2\text{Mn}_{1.4}\text{In}_{0.6}$.

Atom	Wyckoff position	Modulation amplitude	x	y	z	$U_{iso} (\text{\AA}^2)$
Ni1	$4h$		0.5	0.25	0	0.0002(5)
Mn1	$2a$		0	0	0	0.0002(5)
In1	$2d$		0	0.5	0	0.0002(5)
Mn2	$2d$		0	0.5	0	0.0002(5)
		A_1	0.1275(9)	0	0.005(1)	
		B_1	0	0	0	
		A_2	0.0377(17)	0	0.004(2)	
		B_2	0	0	0	